RSC Sustainability

ROYAL SOCIETY OF CHEMISTRY

PAPER

View Article Online
View Journal | View Issue

Cite this: *RSC Sustainability*, 2025, **3**, 3121

Investigation of a sulfonic acid functionalized ammonium-based permanganate hybrid as a sustainable oxidative catalyst for selective conversion of organic sulfides to sulfoxides†

Sangeeta Kalita, Niharika Kashyap, Prapti Priyam Handique, Debanga Bhusan Bora and Ruli Borah *

Received 3rd December 2024
Accepted 28th May 2025

DOI: 10.1039/d4su00760c

rsc.li/rscsus

In this report, two organic–inorganic hybrids of permanganate anions, namely *N*,*N*′-diethyldisulfoammonium permanganate [DEDSA][MnO_4] and 1,4-disulfopiperazinium permanganate [DSPZ][MnO_4]$_2$, were developed as thermally stable oxidants through ion exchange reactions of the respective organic chlorides with a $KMnO_4$ salt. Various spectroscopic and analytical techniques like FT-IR, PXRD, Raman, UV-vis DRS, SEM and EDX were employed to confirm the structural compositions of both the hybrids. Comparative thermogravimetric analyses with reference to the parent organic chloride salts expressed substantial changes in their thermal stabilities as well as their hydrophilic/hydrophobic properties. The oxidative ability of [DEDSA][MnO_4] was observed through its use as an efficient recyclable homogeneous catalyst for selective formation of sulfoxides from aryl/alkyl aryl sulfides in 10% aqueous sulfuric solution at 80 °C for 40–120 min of reaction, resulting in 67–98% yields of products.

Sustainability spotlight

Development of sustainable oxidative catalysts helps to reduce pollution by replacing conventional toxic oxidative reagents, minimizing the formation of over-oxidation products, generating benign by-products, producing clean fuel, and converting waste material to valuable compounds and materials. In this report, a sustainable permanganate-based organic–inorganic hybrid oxidative material is developed by the anion exchange reaction of $KMnO_4$ with a sulfonic-acid-functionalized organic ammonium-based chloride, which efficiently works as a recyclable oxidative catalyst for selective conversion of organic sulphides to sulphoxides in aqueous acidic solution. Thus, our work can help to fulfil Sustainable Development Goals (SDGs) 6, 7 and 12 of the United Nations.

1. Introduction

The oxidation of sulfides is an industrially important organic reaction to prepare sulfoxides and sulfones as key intermediates towards the development of a wide variety of value-added chemical and biological products.[1–6] Most chiral sulfoxides or sulfones are widely used as auxiliaries in asymmetric synthesis that possess high biological activity[7,8] or as ligands in the formation of metal complexes.[9] Likewise, allylic sulfoxides[10] and cyclic sulfoxides/sulfones are utilized as reaction intermediates for designing drug molecules.[11] Furthermore, dimethyl sulfoxide is extensively utilized as a reaction medium and analytical solvent and as a multipurpose reactant.[12,13] It has been observed that the oxidative desulfurization of sterically hindered organic sulphides such as 4,6-dimethyldibenzothiophene (4,6-DMDBT) present in transportation fuel could be performed under mild conditions[14–16] compared to the severe reaction conditions employed in hydrodesulfurization reactions,[17] which include the consumption of excess hydrogen gas at high pressure (approx. 50–100 bar) and temperature (around 643 K) with a notable increase in operational cost. Many reported methods of sulfide oxidation are not satisfactory when performed with stoichiometric amounts of reagents due to unfavourable over-oxidized by-product formation, thus making them unfit for large-scale syntheses.[18–21] Therefore, it is very essential to develop environmentally benign sulfide oxidation routes involving greener oxidants,[22] catalysts[23,24] and solvents[25,26] to overcome the different limitations of traditional reagents for sulfide oxidation[27] for large-scale applications.

Few environmentally benign oxidative systems have been developed for sulfide oxidation using hydrogen peroxide as a greener oxidant in ionic liquids and producing sulfoxides selectively under mild reaction conditions.[17,28,29] Some metal-containing organic salts, particularly polyoxometalate hybrids of organic cations, were also investigated as recyclable and selective oxidative catalysts for sulfide oxidation.[30–35] Among the various types of metal-based oxidants,[36–39] potassium

Department of Chemical Sciences, Tezpur University, Napaam-784028, Tezpur, Assam, India. E-mail: ruli@tezu.ernet.in

† Electronic supplementary information (ESI) available. See DOI: https://doi.org/10.1039/d4su00760c

permanganate is known to be an effective oxidant in organic chemistry for its easy availability and cost-efficiency.[40] Non-selective sulfide oxidation was reported by Bordwell *et al.* in 1952 using an excess amount of $KMnO_4$ in basic aqueous solution under reflux to generate poor to moderate yields of sulfones.[41] Later, Banerji (1988) oxidized a few organic sulfides to the corresponding sulfoxides with $KMnO_4$ *via* a single-step electrophilic shift of the oxygen atom from the permanganate anion and further studied the kinetics of the oxidation reactions.[42] Lee and his co-worker also carried out a mechanistic study of the oxidation of (phenylthio)acetic acid to (phenylsulfonyl)acetic acid in basic solution with an excess amount of $KMnO_4$ to get moderate yields of products.[43] Shaabani *et al.* carried out the oxidation of sulfides with $KMnO_4$, where sulfoxide products were formed in CH_3CN solvent and disulfides were formed in CH_2Cl_2 solvent.[44] To get more insight into the mechanism of sulfide oxidation by $KMnO_4$, Jayaraman and his team conducted theoretical calculations that demonstrated a mechanism involving the 1,3-dipolar cycloaddition of permanganate.[45] Improvement of the non-selective nature of $KMnO_4$-based sulfide oxidation was observed after heterogenization of potassium permanganate in the form of solid-supported reagents, such as $KMnO_4$/alumina,[46] $KMnO_4$/MnO_2,[47] $KMnO_4$/montmorillonite K10,[48] $KMnO_4$/$MnSO_4 \cdot H_2O$.[49] However, most of these methods used excess amounts of $KMnO_4$/solid support reagents and had longer reaction times (1–20 h), pointing towards the lower reactivity of these systems in oxidation reactions.

Eventually, the selective oxidative of organic sulfides to sulfones was also studied using organic–inorganic hybrids of permanganate oxidants,[50] such as benzyltriethylammonium permanganate,[51,52] methyltriphenylphosphonium permanganate[53] and tetra-*n*-butylammonium permanganate[54] at lower temperatures in organic solvents. However, these ammonium permanganates were unstable above ambient temperature and required freshly prepared reagents and careful handling due to their explosive nature and lack of storability. Lakouraj *et al.* developed *N*,*N*′-dibenzyl-*N*,*N*,*N*′,*N*′-tetramethyl diammonium permanganate (DBTMEP) as a thermally stable reagent up to 110 °C, and used it in the selective conversion of sulfides to sulfones,[55] although it decomposes violently during harsh grinding.

Considering the circumstances, a viable organic–inorganic hybrid of a permanganate anion with an organic cation could be synthesized by the ion exchange reaction of N–SO_3H-functionalized cyclic/acyclic-ammonium-based ionic liquids of chloride anions with permanganate anions of $KMnO_4$. It is well known that organic salts of organic or inorganic anions tethered with –COOH and –SO_3H groups in organic cations have been developed as task-specific ionic liquids if their melting points are below 100 °C and they possess all the unique physicochemical properties of ionic liquids for further use as functional materials in different fields.[56–59] By incorporating sulfonic groups into the organic cation of a permanganate hybrid, one could expect strong electrostatic interactions between the ion pair, involving intra-molecular H-bonding interactions of –OH groups of sulfonic acid with the oxygen atoms of permanganate

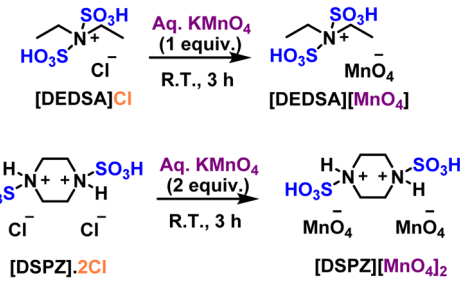

Scheme 1 The synthesis of permanganate hybrids of –SO_3H-functionalized diethylammonium/piperazinium cations.

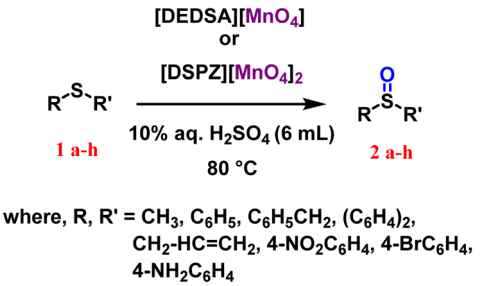

Scheme 2 The selective oxidation of sulfides to sulfoxides by the permanganate hybrids.

anions. In addition to that, possible intermolecular H-bonding interactions between the cations of permanganate hybrids *via* sulfonic groups may tightly pack all molecules into a rigid material with higher thermal stability.

Extending our previous work on the catalytic performance of various organic–inorganic hybrids based on task-specific ionic liquids,[60,61] we focus on synthesizing a mono-cationic *N*,*N*′-diethyldisulfoammonium organic salt ($[DEDSA]^+$) and a di-cationic 1,4-disulfopiperazinium organic salt ($[DSPZ]^{2+}$) with permanganate as the anion, as seen in Scheme 1. In both cases, the synthetic procedures involve ion exchange between the reported precursor ionic liquid/salt ([DEDSA]Cl and [DSPZ]·2Cl) and an aqueous solution of potassium permanganate, respectively. After confirming the compositions of both hybrids using various analytical tools, their oxidizing capacities were explored through their use as reusable homogeneous catalysts for the selective oxidation of organic sulfides to sulfoxides (Scheme 2) in aqueous solutions of sulfuric acid under reflux conditions.

2. Materials and methods

2.1. Materials

The required chemicals were purchased from reputable and reliable chemical companies like Merck, Loba Chemie, SRL and Tokyo Chemicals with the highest purity.

2.2. Methods

FT-IR spectra were recorded on a PerkinElmer MIR-FIR FT-IR spectrophotometer. A JEOL 400 MHz spectrophotometer (δ in ppm) was employed to obtain the ^1H NMR and ^{13}C NMR spectra

of precursor ionic liquids/salts with DMSO-d_6 as solvent (Fig S1–S4†). The same spectrophotometer was used to obtain the ^{1}H and ^{13}C NMR spectra of isolated sulfoxide products (Table S1†). Thermo-gravimetric analyses (TGA) of the organic salts of chloride anions and permanganate anions were conducted up to 600 °C on Shimadzu TGA-50 apparatus, while UV-diffuse reflectance spectra (DRS) of the organic salts of permanganate anions within a wavelength range of 200–800 nm were attained using a Shimadzu UV 2450 spectrophotometer. PXRD diffraction patterns were obtained using a 9-KW powder X-ray diffraction system (make: Rigaku technologies, Japan; model: Smart Lab). Scanning electron microscopy (SEM) images as well as energy dispersive X-ray (EDX) images were collected using a JEOL JSM-6390LV SEM. Raman spectroscopy analyses of the hybrids were performed on a RENISHAW BASIS SERIES spectrophotometer furnished with a green argon-ion laser with an excitation wavelength of 514.5 nm. The nitrogen adsorption–desorption isotherm analysis was performed by the Brunauer–Emmett–Teller (BET) method to obtain the average surface area and pore volume of the hybrids (Quantachrome; model: Autosorb-IQ MP). Product analysis was carried out by gas chromatography-mass spectrometry (GC-MS) on PerkinElmer Clarus 680 apparatus with a 5 MS (methyl polysiloxane) column (60.0 m × 250 μm) using He as the carrier gas (flow rate: 1 mL min^{-1}). The injector temperature and source temperature were 250 °C and 160 °C, respectively, while the column temperature was 60–300 °C. The GC oven was operated with an initial temperature of 60 °C for 1 min, and this was raised up to 200 °C at a rate of 7 °C min^{-1} (hold time: 3 min), before being further raised up to 300 °C at a rate of 10 °C min^{-1} (hold time: 5 min).

2.3. Synthesis of *N*,*N*′-diethyldisulfoammonium permanganate ([DEDSA][MnO_4]) and 1,4-disulfopiperazinium permanganate ([DSPZ][MnO_4]$_2$) hybrids

The *N*,*N*′-diethyldisulfoammonium permanganate ([DEDSA][MnO_4]) hybrid was prepared *via* the formation of a precursor *N*,*N*′-diethyldisulfoammonium chloride ([DEDSA]Cl) ionic liquid, which was subjected to an anion exchange reaction with $KMnO_4$ (Scheme 1). Firstly, 10 mmol of diethylamine in 30 mL of dry hexane was combined with 20 mmol of chlorosulfonic acid at room temperature for 1 h, as per the standard procedure, to get 96% yield of [DEDSA]Cl as a brown viscous liquid.[62] 9 mmol of the resultant [DEDSA]Cl ionic liquid was then added dropwise to 9 mmol of aqueous $KMnO_4$ (in 30 mL of distilled water) solution under continuous stirring at room temperature for the exchange reaction of chloride anions with permanganate anions to occur. The reaction was stirred for 3 h and the brownish-black precipitate of the permanganate hybrid of ammonium cations was collected by centrifugation, washed thoroughly with distilled water and dried under vacuum at 80 °C for 24 h to obtain 95% yield of the [DEDSA][MnO_4] hybrid.

Similarly, the anion exchange reaction of 1,4-disulfopiperazinium chloride ([DSPZ]·2Cl) salt with permanganate anions was carried out with an aqueous solution of $KMnO_4$ to get the 1,4-disulfopiperazinium permanganate hybrid ([DSPZ][MnO_4]$_2$) (Scheme 1). To start this process, 20 mmol of chlorosulfonic acid was added dropwise to a solution of 10 mmol of piperazine in dry CH_2Cl_2 in a 100 mL round-bottom flask at room temperature, according to the reported literature, which produced 95% yield of the [DSPZ]·2Cl ionic salt as a white solid after stirring for 1 h.[63] The exchange of the chloride anions of this organic salt with permanganate anions took place when 9 mmol of [DSPZ]·2Cl was reacted with 18 mmol of aqueous $KMnO_4$ solution at room temperature for 3 h. The reaction mixture was centrifuged and washed thoroughly with distilled water. After drying the precipitate at 80 °C in a vacuum oven, the brownish-black precipitate was collected with 94% yield of the [DSPZ][MnO_4]$_2$ hybrid.

2.4. Typical method for the oxidation of organic sulfides to sulfoxides using [DEDSA][MnO_4] as catalyst

For the oxidation of sulfides to sulfoxides, 1 mmol of the organic sulfide compound was taken in a 100 mL two-necked round-bottom flask containing 6 mL of 10% aqueous sulfuric acid solution (Scheme 2). Then the reaction mixture was stirred at 80 °C under reflux conditions for the specified reaction time after the addition of 20 mol% [DEDSA][MnO_4] catalyst until the reaction was completed as monitored by the thin layer chromatographic technique (TLC). After that, the product was extracted from acidic aqueous solution with dichloromethane (3 × 5 mL) and dried over anhydrous sodium sulfate. Evaporation of the dichloromethane extract under reduced pressure produced the crude sulfoxide product for GC-MS analysis. The yield (%) of sulfoxide was attained after purification of the crude product using column chromatography. Subsequently, the used permanganate catalyst was recovered from the acidic aqueous layer through precipitation after neutralization with 10% aqueous NaOH solution, and it was then filtered, washed with distilled water and dried in a vacuum oven at 80 °C for reactivation.

3. Results and discussion

3.1. Catalyst characterization

3.1.1. NMR and FT-IR analysis. The two sulfonic-acid-functionalized permanganate hybrids of ammonium cations, *i.e.* *N*,*N*′-diethyldisulfoammonium permanganate ([DEDSA][MnO_4]) and 1,4-disulfopiperazinium permanganate ([DSPZ][MnO_4]$_2$) hybrids, were prepared according to Scheme 1 and then subjected to various analytical techniques for characterization. The existence of organic cations in these hybrids was evidenced from ^{1}H and ^{13}C NMR spectra (Fig S1–4†) of the precursor chloride-based organic salts, *i.e.* [DEDSA]Cl and [DSPZ]·2Cl, due to difficulties relating to the solubilization of the permanganate hybrids of ammonium cations in most common NMR solvents. Furthermore, a comparison between the FT-IR spectra of the synthesized materials and their respective precursor ionic liquids/salts showed the inclusion of organic cations, as indicated by the characteristic vibrational peaks of sulfonic groups attached to both ammonium and piperazinium cations (Fig. 1a and c). In the case of [DEDSA]

[MnO_4] (Fig. 1a), the attached –SO_3H groups showed prominent but overlapping S–O asymmetric and symmetric stretches at 1111 cm^{-1} and 1028 cm^{-1}, along with a sharp S–O bending vibration at 523 cm^{-1} as compared to the same vibrations at 1128 cm^{-1}, 1057 cm^{-1} and 583 cm^{-1}, respectively, for the parent ionic liquid [DEDSA]Cl.[62] The peaks at 712 cm^{-1} and 1457 cm^{-1} were associated with the out-of-plane ring bending vibrations of C–H bonds and bending vibrations of –CH_2 groups, respectively. A weak peak at 830 cm^{-1} occurred due to stretching vibrations of N–S bonds. The physisorbed water molecules along with O–H stretches of –SO_3H groups caused a broad peak around 3000–3500 cm^{-1}, while H–O–H bending vibrations of physisorbed water gave rise to a medium strength peak at 1628 cm^{-1}. Weak stretches around 2800–2900 cm^{-1} were observed due to methyl group C–H stretches. The distinctive peak at 910 cm^{-1} for the MnO_4^- ion was found to overlap with the intense peak of [DEDSA][MnO_4] around 1028–1111 cm^{-1} as an IR active vibration, contrary to its inactive character in the Raman spectrum (Fig. 5c) of the hybrid.[64,65] In the FT-IR spectrum of [DSPZ][MnO_4]$_2$ in Fig. 1c, all the characteristic vibrations of sulfonic group such as S–O asymmetric, symmetric and bending vibrations were observed at 1152 cm^{-1}, 1078 cm^{-1} and 589 cm^{-1}, respectively, compared to their original positions in the precursor salt [DSPZ]·2Cl at 1174 cm^{-1}, 1064 cm^{-1} and 583 cm^{-1}. It also showed a weak peak at 868 cm^{-1} for N–S stretches in addition to two weak peaks at 739 cm^{-1} for out-of-plane ring bending of C–H bonds and at 1444 cm^{-1} for CH_2 group bending vibrations of the piperazine ring.[63] The sharp peak at 1647 cm^{-1} was caused by bending vibrations of N–H bonds, but the broad peaks around 2700–3500 cm^{-1} could be due to overlapping N–H bond stretches, C–H bond stretches and O–H bond stretching vibrations of –SO_3H groups along with intermolecular H-bonded H_2O molecules. The weak peak at 955 cm^{-1} for the MnO_4^- anion was observed in the case of the piperazinium permanganate hybrid, although it was absent in the Raman spectrum of the hybrid (Fig. 5d). Additionally, far-IR analysis showed the appearance of two weak vibrations around 400–500 cm^{-1} in both materials, referring to the ν_4 (F_2) Raman-active mode,[65] which also indicated the inclusion of the permanganate anion in the hybrids, as seen in Fig. 1b for [DEDSA][MnO_4] and Fig. 1d for [DSPZ][MnO_4]$_2$.

3.1.2. Thermogravimetric analysis. Thermogravimetric analysis (TGA) of [DEDSA][MnO_4], as shown in Fig. 2a, expressed its greater hydrophobic nature than the parent ammonium chloride [DEDSA]Cl, as this hybrid didn't lose any physisorbed water around 100 °C, contrary to its precursor [DEDSA]Cl which lost around 14% of physisorbed water (equivalent to 2 molecules of water). Above 150 °C, the hybrid displayed around 2–4% mass loss up to 600 °C that could be attributed to the elimination of crystallized water through the cleavage of strong intermolecular H-bonding interactions involving the sulfonic groups of hybrids. Conversely, the precursor [DEDSA]Cl salt was observed to be thermally stable

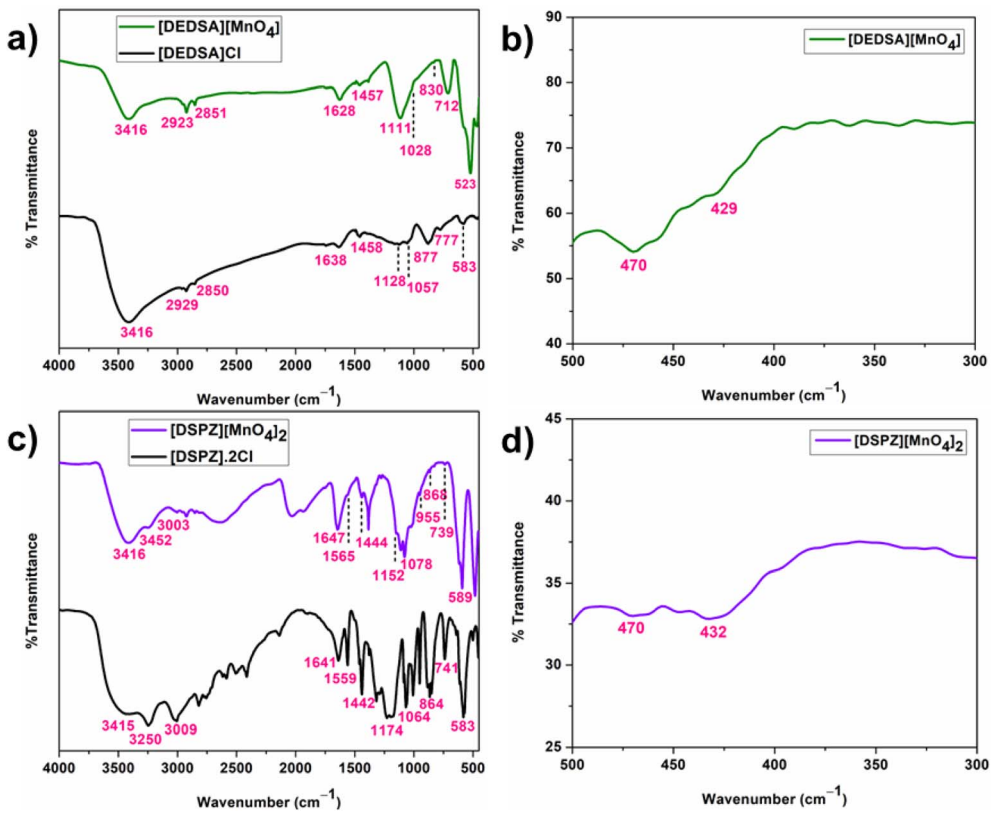

Fig. 1 Comparative FT-IR spectra of (a) [DEDSA]Cl and [DEDSA][MnO_4], (b) far-IR analysis of [DEDSA][MnO_4], (c) comparative FT-IR spectra of [DSPZ]·2Cl and [DSPZ][MnO_4]$_2$, and (d) far-IR analysis of [DSPZ][MnO_4]$_2$.

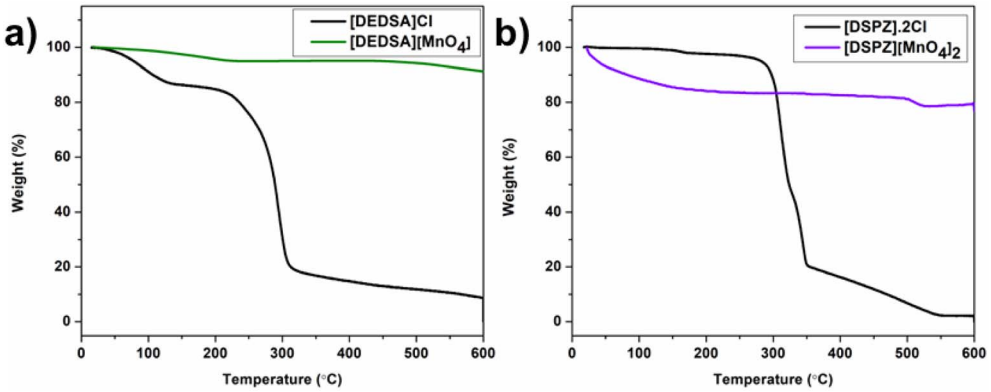

Fig. 2 Comparative thermogravimetric analysis curves of (a) [DEDSA]Cl and $[DEDSA][MnO_4]_2$ and (b) [DSPZ]·2Cl and $[DSPZ][MnO_4]_2$.

only up to 250 °C. Whereas, comparative TGA plots of [DSPZ] $[MnO_4]_2$ and the precursor organic salt [DSPZ]·2Cl showed the increasing hydrophilic properties of the permanganate hybrid, showing gradual loss of 14% physisorbed water up to 100 °C and then continuing to be stable up to 500 °C, as seen in Fig. 2b. In this case, the parent [DSPZ]·2Cl contained almost no physisorbed water but degraded completely above 300 °C.

3.1.3. Scanning electron microscopy (SEM) analysis. SEM images of $[DEDSA][MnO_4]$ (Fig. 3a and b) portrayed aggregated crystalline structures of almost similar size. The morphological specifics of the SEM images indicated the formation of agglomerates of medium-scale crystals, with an average size of 1.79 μm. However, the presence of inconsistently sized crystals could be seen in SEM images of $[DSPZ][MnO_4]_2$ (Fig. 3d and e). These slightly larger irregularly sized crystals, with an average size of 2.88 μm, formed heterogeneous surface agglomerates. Both hybrids contained needle-like particles over the crystal surfaces, which could be clearly seen in SEM images of the salts with higher resolution (Fig. 3b and e). The presence of intermolecular interactions within the systems could be responsible for the development of the aggregates in these salts. The formation of extensive networks of H-bonding could be possible in these hybrids, owing to the polarized $-SO_3H$ groups attached to the ammonium moieties, which would significantly contribute to the heterogeneity in both the permanganate hybrids. Besides, the continuous presence of oppositely charged cations and anions could also lead to the formation of ion–ion or ion–dipole interactions in the molecular arrangement, which could enhance the rigidity of the synthesized materials.

3.1.4. Energy dispersive X-ray analysis. Energy dispersive X-ray (EDX) analysis of the two organic salts (Fig. 3c and f) depicted the presence of all the expected elements. Based on the EDX analysis, the existence of any undesired impurities was also ruled out.

3.1.5. Powder X-ray diffraction pattern analysis. Powder X-ray diffraction (PXRD) patterns (Fig. 4) of the hybrid organic salts exhibited a primitive lattice configuration, as observed in the case of $KMnO_4$. However, variations in the peak intensities in the XRD patterns of the hybrids were noticed after the smaller K^+ cation was substituted with bulkier ammonium or

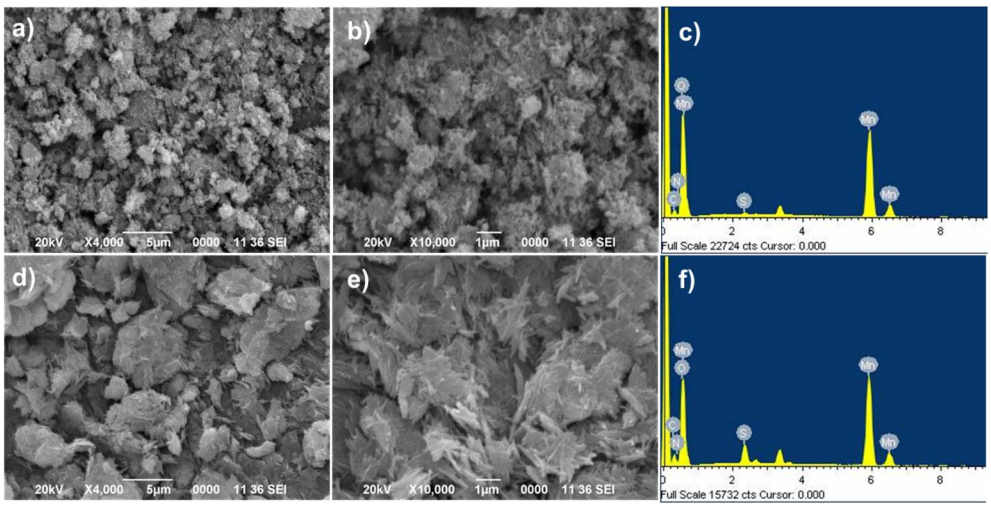

Fig. 3 (a and b) SEM images of $[DEDSA][MnO_4]$, (c) EDX analysis of $[DEDSA][MnO_4]$, (d and e) SEM images of $[DSPZ][MnO_4]_2$, and (f) EDX analysis of $[DSPZ][MnO_4]_2$.

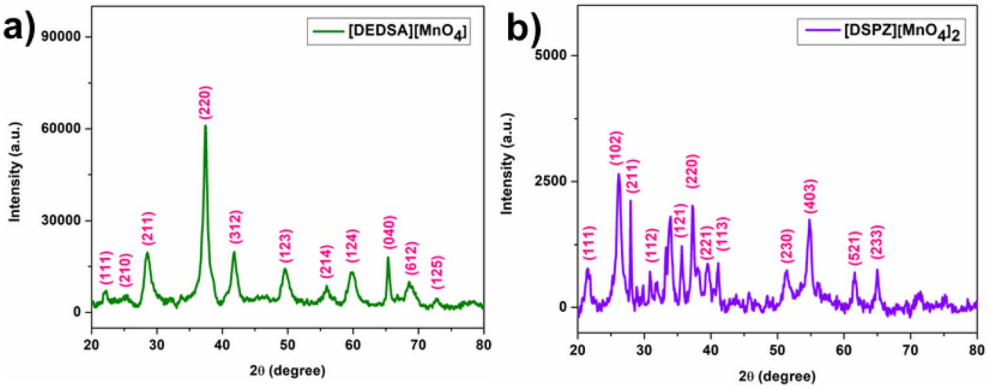

Fig. 4 PXRD patterns of (a) [DEDSA][MnO_4] and (b) [DSPZ][MnO_4]$_2$.

piperazinium cations functionalized with sulfonic acid groups. Additionally, the 2θ value of the most profound $KMnO_4$ peak at 27.78°, in line with JCPDS card no. 89-3951, was found to be altered for both [DEDSA][MnO_4] and [DSPZ][MnO_4]$_2$. These changes could be the aftermath of introducing sulfonic-acid-functionalized organic cations to permanganate anions, as they were likely to be involved in possible inter/intra-molecular H-bonding, as well as electrostatic interactions, including ion–ion or ion–dipole interactions in these hybrids.

For the ammonium-based hybrid, peaks with 2θ values of 22.16°, 25.46°, 28.54°, 37.43°, 41.82°, 49.62°, 55.61°, 59.80°, 65.39°, 68.87° and 72.67° represented the (111), (210), (211), (220), (312), (123), (214), (124), (040), (612) and (125) reflection planes, respectively. For the piperazinium-based hybrid, peaks with 2θ values of 21.46°, 26.15°, 27.95°, 30.84°, 35.63°, 37.23°, 39.53°, 41.12°, 51.41°, 54.79°, 61.59° and 64.99° were assigned to the (111), (102), (211), (112), (121), (220), (221), (113), (230), (403), (521) and (233) reflection planes, respectively.

3.1.6. UV-visible diffuse reflectance spectra analysis. The UV-visible diffuse reflectance (DRS) spectra of both hybrids (Fig. 5a and b) were correlated with that of $KMnO_4$ (Fig. S5†). In the case of [DEDSA][MnO_4], the UV-DRS spectrum showed absorption peaks at around 224 nm and 301 nm, denoting the $^1A_1 \rightarrow {}^1T_2$ ($t_1 \rightarrow 4t_2$) electronic transition and $^1A_1 \rightarrow {}^1T_2$ ($3t_2 \rightarrow$

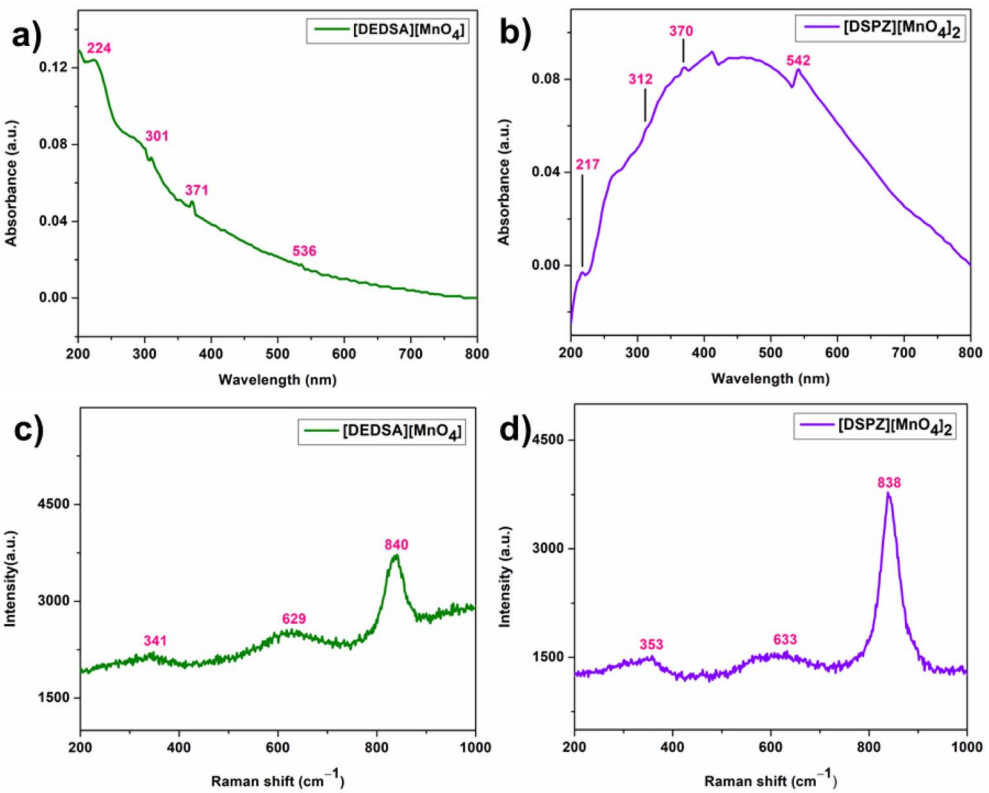

Fig. 5 UV-DRS spectra of (a) [DEDSA][MnO_4] and (b) [DSPZ][MnO_4]$_2$; Raman spectra of (c) [DEDSA][MnO_4] and (d) [DSPZ][MnO_4]$_2$.

2e) transition, respectively, of the permanganate anion.[66] The broad and very weak shoulder peak at around 536 nm was due to the $^1A_1 \rightarrow {}^1T_2$ ($t_1 \rightarrow 2e$) transition of the MnO_4^- anion, whereas the weak-intensity peak at 371 nm could be assigned to the $^1A_1 \rightarrow {}^1T_1$ ($3t_2 \rightarrow 2e$) orbitally forbidden transition. Another forbidden low-intensity peak from the $^1A_1 \rightarrow {}^1T_1$ ($t_1 \rightarrow 2e$) transition at around 690 nm was undefined for both the synthesized hybrids. All these transitions also appeared in the case of the permanganate hybrid of the piperazinium cation with somewhat altered wavelength values. The intensities of these absorptions in the hybrids were notably reduced compared to those in $KMnO_4$, which could be due to the diverse electronic states of MnO_4^- anions in the synthesized materials. The reason behind this was anticipated to be the formation of strong networks of H-bonding among the oxygen atoms of MnO_4^- anions and sulfonic acid groups attached to the ammonium or piperazinium cations, which were absent in $KMnO_4$ due to the smaller size of the K^+ cation, resulting in discrete electronic transitions, contrary to the synthesized materials.[67]

3.1.7. Raman spectroscopy analysis. Raman spectra of both the synthesized ammonium- and piperazinium-based hybrids showed intense peaks at 840 cm^{-1} and 838 cm^{-1} (Fig. 5c and d), which were in accordance with the distinctive peak of the MnO_4^- anion at 840 cm^{-1} for the ν_1 (A_1) symmetric 'breathing' mode (Fig. S6†).[68] However, the intensity of this vibration was reduced in the case of the [DEDSA][MnO_4] peak compared to that in both its piperazinium analogue and $KMnO_4$. The absence of ν_3 (F_2) mode vibrations in both the synthesized salts was blamed on the distorted tetrahedral structure of the MnO_4^- anion, which was probably caused by the formation of H-bonding along with inter/intra-ionic interactions in these hybrids, as mentioned earlier. The very weakly active ν_4 (F_2) Raman vibrations within the range of 400–500 cm^{-1} were missing,[65] contrary to their appearance in the far-IR spectra of the hybrids (Fig. 1b and d). Weak vibrations around 341 cm^{-1} and 353 cm^{-1} were seen for the ammonium and piperazinium hybrids, respectively, like that in the precursor $KMnO_4$. In addition, a small amount of MnO_2 was found to be mixed along with MnO_4^- anions in the hybrids, as portrayed by the impurity peaks near 630 cm^{-1} for the organic salts.

3.1.8. Brunauer–Emmett–Teller (BET) analysis. The Brunauer–Emmett–Teller (BET) isotherm plots of [DEDSA][MnO_4] and [DSPZ][MnO_4]$_2$ materials from N_2 gas adsorption–desorption provided findings about their specific surface areas, pore volumes and pore diameters (Fig. 6). The mesoporous nature of the materials was indicated by the typical type-IV isotherms in both cases.[69] The specific surface area of [DSPZ][MnO_4]$_2$ was found to be 239.209 $m^2\ g^{-1}$, which was almost twice the specific surface area of [DEDSA][MnO_4] (122.216 $m^2\ g^{-1}$). The pore volume of [DSPZ][MnO_4]$_2$ was observed to be more than two times that of [DEDSA][MnO_4], precisely 0.181 $cm^3\ g^{-1}$ for [DEDSA][MnO_4] and 0.505 $cm^3\ g^{-1}$ for [DSPZ][MnO_4]$_2$. The pore size distribution over the surfaces of both the materials was revealed by the Barrett–Joyner–Halenda (BJH) curves, as shown in the insets of Fig. 6, where ~2–20 nm was found to be the prime range for the hybrid materials. The pore diameters of the [DEDSA][MnO_4] and [DSPZ][MnO_4]$_2$ materials were identified as 3.741 nm and 7.059 nm, respectively, as observed from the BJH plots of the materials.

3.2. Catalytic study

3.2.1. Optimization of reaction conditions. The oxidative performances of the synthesized sulfonic-acid-tethered ammonium-based permanganate hybrids were studied through their use as recyclable oxidative catalysts for the selective conversion of organic sulfides to sulfoxides in aqueous sulfuric acid solution and in aqueous solutions of sulfuric acid with polar organic solvents like acetonitrile (CH_3CN), ethyl acetate (EtOAc) and glacial acetic acid at different temperatures. For this purpose, thioanisole was selected as a model organic sulfide to optimize the reaction conditions for sulfide oxidation, like screening the solvent, amount of oxidative catalyst and reaction temperature. Initially, a model reaction with thioanisole (1 mmol) was conducted in acetonitrile and ethyl acetate (6 mL) under reflux temperatures using 20 mol% [DEDSA][MnO_4] as a heterogeneous catalyst for 2 h, which didn't give any product (Table 1, entries 1 and 2). Interestingly, the same amount of catalyst produced excellent yield (93%) of sulfoxide within 40 min in 10% H_2SO_4 solution (6 mL) at 80 °C in a homogeneous phase (Table 1, entry 3). However, when a 1 : 1

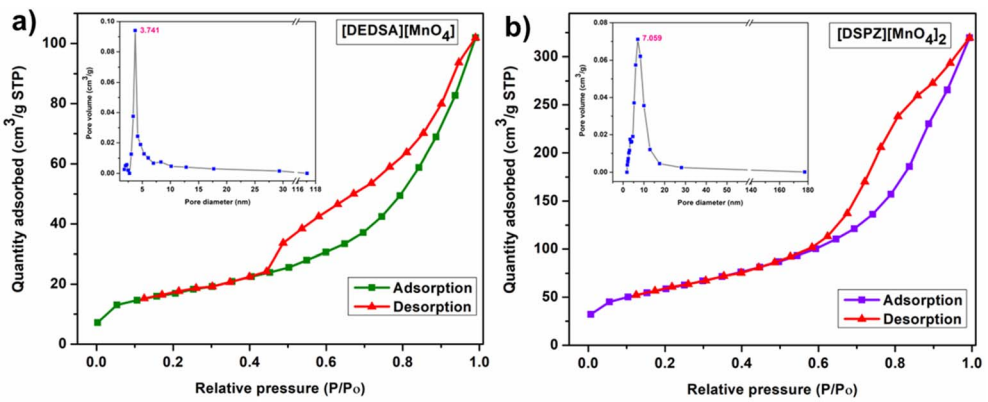

Fig. 6 BET isotherms and BJH plots (insets) of (a) [DEDSA][MnO_4] and (b) [DSPZ][MnO_4]$_2$.

mixture of acetonitrile and 10% H_2SO_4 solution was used, a decent yield (79%) of the desired sulfoxide product was obtained (Table 1, entry 4) in 45 min of reaction time. Conducting the model reaction in a biphasic 1 : 1 mixture of EtOAc and 10% H_2SO_4 solution at 75 °C gave only a trace amount of sulfoxide in 2 h (Table 1, entry 5). In glacial acetic acid at 80 °C, the reaction gave sulfone as a major over-oxidized product along with minor amounts of sulfoxide and unreacted sulfide (Table 1, entry 6). The use of aqueous nitric acid at a pH of 1 in place of sulfuric acid also produced 77% yield of the product under homogeneous conditions with 20 mol% catalyst at 80 °C after 2 h of reaction (Table 1, entry 7). However, using phosphoric acid solution at the same pH showed only 61% yield of the sulfoxide after 2 h of reaction, which could be expected due to the heterogeneous phases of the reaction mixture in acidic solution (Table 1, entry 8). Then, increasing the catalyst amount to 30 mol% in 10% H_2SO_4 solution at 80 °C with 45 min of reaction led to the formation of the over-oxidized product of sulfoxide (Table 1, entry 9). However, reducing the catalyst amount to 10 mol% resulted in the inadequate conversion of substrate 1a into the sulfoxide (Table 1, entry 10) after 2 h of reaction. The yields of sulfoxide were reduced in 10% H_2SO_4 solution when the reaction was performed at 50 °C and room temperature for 2 h (Table 1, entries 11–12). 20 mol% catalyst was also examined for the $[DSPZ][MnO_4]_2$ hybrid in 10% H_2SO_4 solution at 80 °C which showed poor results (Table 1, entry 13). Thereafter, the substrate scope study for various sulfide compounds was carried out using 20 mol% [DEDSA][MnO_4] in 10% H_2SO_4 at 80 °C. To study the catalytic effects of the two precursor organic salts [DEDSA]Cl and [DSPZ]·2Cl, the model reaction was also conducted under the optimized conditions using these salts at 20 mol% as catalysts for 2 h at 80 °C (Table 1, entries 14 and 15). No reactions occurred in both cases, which supported the catalytic role of the permanganate anion as per the proposed mechanism in acidic solution.

3.2.2. Substrate scope study. The substrate scope study for the selective oxidation of sulfides under the optimized conditions (Fig. 7) showed that sulfides such as thioanisole, diphenyl sulfide and benzyl phenyl sulfide produced excellent yields of the corresponding sulfoxide products (>90%) within an hour of reaction time. Dibenzothiophene also generated satisfactory product yield in a relatively longer reaction span. In the case of allyl phenyl sulfide, the formation of allyl phenyl sulfoxide with 77% yield showed the chemoselective nature of the catalyst. However, the presence of a small amount of the dihydroxylated product was also detected along with the major sulfoxide product. Regarding the substituted thioanisoles, 4-nitrothioanisole and 4-bromothioanisole produced reasonable yields of sulfoxides, but 4-(methylthio)aniline showed no reaction after up to 2 h of reaction time. An aliphatic sulfide was inactive for the oxidation reaction, as observed for the oxidation of dihexyl sulfide, and did not produce any product after 3 h of reaction under the optimized conditions.

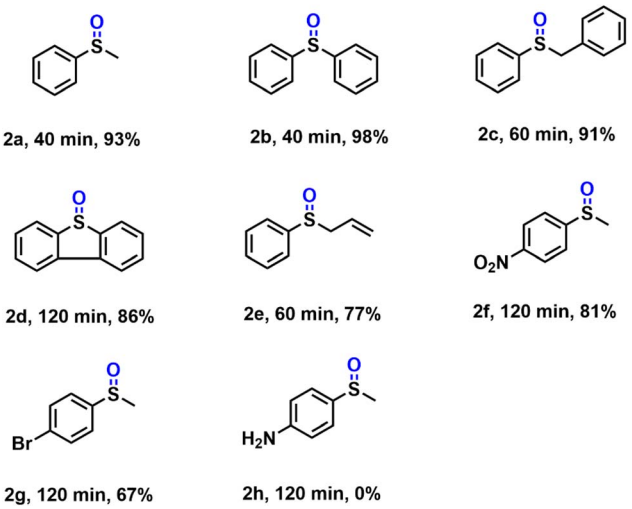

Fig. 7 The oxidation of organic sulfides under the optimized conditions using 20 mol% [DEDSA][MnO_4] catalyst.

Table 1 Optimization of the model reaction for sulfide oxidation using the [DEDSA][MnO_4] hybrid catalyst

Entry	Catalyst	Catalyst amount (mol%)	Solvent	Temp. (°C)	Time[a] (min)	pH	% Yield[b] (**2a**)
1	[DEDSA][MnO_4]	20	CH_3CN	80	120	—	—
2	[DEDSA][MnO_4]	20	EtOAc	80	120	—	—
3	[DEDSA][MnO_4]	20	10% H_2SO_4	80	40	1	93
4	[DEDSA][MnO_4]	20	CH_3CN + 10% H_2SO_4	80	45	1	79
5	[DEDSA][MnO_4]	20	EtOAc + 10% H_2SO_4	75	120	1	Trace
6	[DEDSA][MnO_4]	20	Glacial acetic acid	80	120	3	22[c]
7	[DEDSA][MnO_4]	20	10% HNO_3	80	120	1	77
8	[DEDSA][MnO_4]	20	10% H_3PO_4	80	120	1	61
9	[DEDSA][MnO_4]	30	10% H_2SO_4	80	45	1	80
10	[DEDSA][MnO_4]	10	10% H_2SO_4	80	120	1	61
11	[DEDSA][MnO_4]	20	10% H_2SO_4	50	120	1	79
12	[DEDSA][MnO_4]	20	10% H_2SO_4	R.T.	120	1	67
13	$[DSPZ][MnO_4]_2$	20	10% H_2SO_4	80	45	1	38
14	[DEDSA]Cl	20	10% H_2SO_4	80	120	1	—
15	[DSPZ]·2Cl	20	10% H_2SO_4	80	120	1	—

[a] Using 1 mmol of thioanisole as the model substrate. [b] Isolated yield. [c] Major product sulfone (61% yield).

Table 2 A comparison of the model reaction in the present work with earlier reports of sulfide oxidation

Entry	Solvent	Catalyst	Oxidant	Temp. (°C)	Time	% Yield [ref.]
1	[Bmim][BF_4]	—	H_2O_2 (20 mmol)	25	4 h	95 (ref. 28)
2	H_2O	$Mn(OAc)_2$/[C_{12}mim][NO_3] (0.2 mol/20 mL)	Molecular oxygen (50 mL min^{-1})	50	2 h	97 (ref. 70)
3	—	[Hmim]HSO_4 (2 mmol)	Ceric ammonium nitrate (CAN) (1 mmol)	80	5 min	94 (ref. 71)
4	CH_3CN	$VO_2F(dmpz)_2$ (0.02 mmol)	H_2O_2 (2.2 mmol)	0–5	5 h	95 (ref. 72)
5	2,2,2-Trifluoroethanol (TFE)	$Fe(NO_3)_3 \cdot 9H_2O$ (5 mol%)	O_2 (0.2 MPa)	80	4 h	95 (ref. 73)
6	CH_3CN	Ru(PVP)/γ-Al_2O_3 (0.5 mmol)	H_2O_2 (1 mmol)	R.T.	120 min	98 (ref. 74)
7	10% H_2SO_4	[DEDSA][MnO_4] (20 mol%)	—	80	40 min	93 this work

A comparative study was performed between the present work and earlier reports, as shown in Table 2, which showed the better sustainability of this catalytic system in an aqueous solution of sulfuric acid without the use of any external oxidants for the controlled oxidation of the sulfide, where sulfuric acid acted as a co-catalyst according to the proposed mechanism.

3.3. Plausible mechanism

A plausible mechanism for sulfide oxidation catalyzed by the [DEDSA][MnO_4] hybrid is illustrated in Scheme 3 for the model substrate (**1a**) in acidic solution. In an acidic environment, the permanganate anion of the hybrid catalyst **I** undergoes protonation and thereby acts as an electron-deficient metal center in intermediate **II** along with HSO_4^- as a counter anion. Then, nucleophilic attack by thioanisole (**1a**) of the metal center of intermediate **II** occurs and leads to the formation of intermediate **III**. Thereafter, the HSO_4^--initiated proton abstraction and hydrolysis of intermediate **III** could be expected, involving nucleophilic attack by a water molecule of the electrophilic S atom of intermediate **III**, followed by cleavage of the Mn–S bond

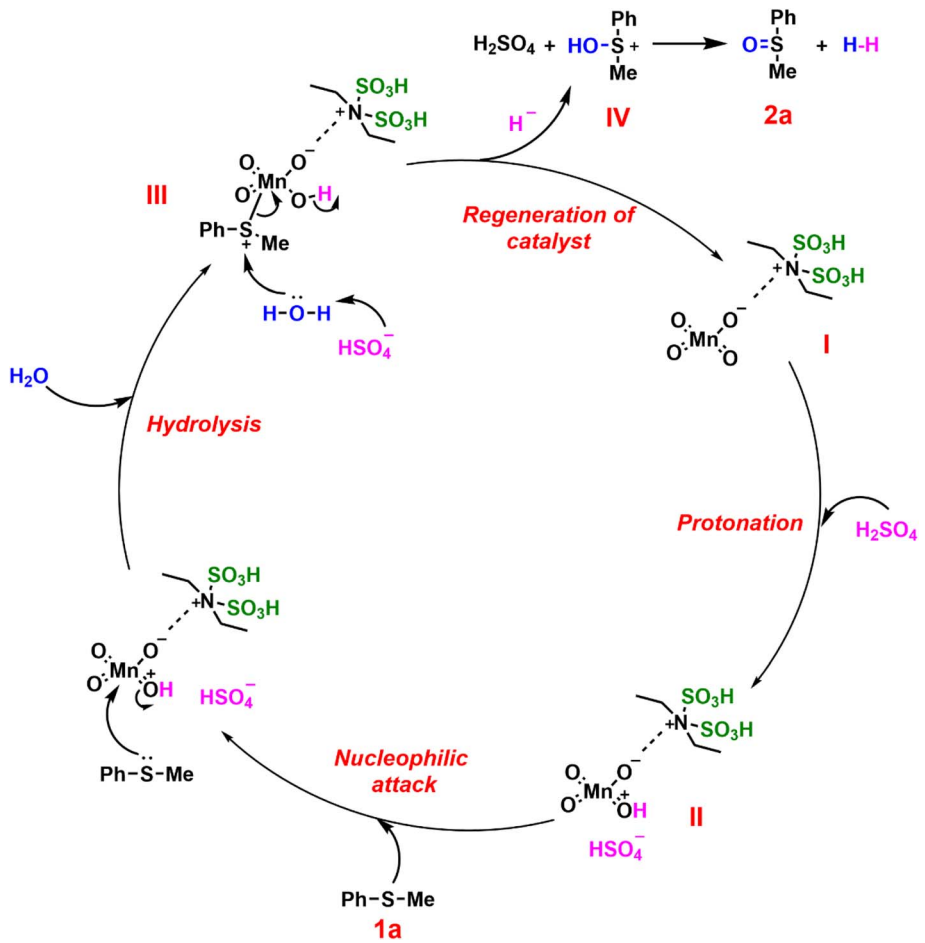

Scheme 3 A plausible mechanism for the oxidation of sulfides to sulfoxides with the [DEDSA][MnO_4] salt.

along with the elimination of a H^- anion as a hydrogen molecule in acidic solution, which regenerates the permanganate hybrid **I**. Finally, the sulfonium intermediate **IV** yields the sulfoxide product after releasing the acidic proton to the reaction medium. Again, the participation of water molecules in the supply of oxygen atoms for sulfoxide formation was evidenced by conducting the model reaction under a nitrogen atmosphere which showed an identical result to the presence of atmospheric oxygen molecules.

3.4. Catalyst recyclability

The recyclability of the [DEDSA][MnO_4] oxidative catalyst was examined on the 3 mmol scale using the model substrate after the successful execution of the 1st reaction under the optimized reaction conditions. To recover the used catalyst from the aqueous 10% H_2SO_4 layer after the extraction of the sulfoxide product in organic extract, as mentioned in the experimental procedure, 10% NaOH solution was added dropwise to neutralize the aqueous acidic solution for the complete precipitation of the permanganate hybrid in one hour. The precipitate was then collected by centrifugation and washed with distilled water (3 times) as well as acetone (2 times). After drying it under vacuum for 24 h, the recovered catalyst was obtained, which was further analyzed using FT-IR, P-XRD and EDX to check its integrity before subjecting it to another reaction cycle. The catalyst could be used for up to four consecutive reaction cycles, although a significant decrease in product yield after a comparable reaction time was observed after each cycle (Fig. 8a). The reason behind this could be the probable loss of catalyst activity owing to its repeated washing and drying under vacuum after each cycle, with the formation of a small amount of Mn(II) salts due to the slow reactions of permanganate anions with sulfuric acid and sodium hydroxide solution under the reaction conditions. The existence of additional small peaks at 32.5° and 58° in the PXRD spectrum of the reused catalyst after the 4th cycle displayed the presence of small amounts of $MnSO_4$ and MnO_2 impurities, as per JCPDS card no. 85-0425 and card no. 89-5171, respectively (Fig. 8b). The FT-IR spectrum of the recovered catalyst showed the retention of most absorbance peaks exhibited by the fresh catalyst with slightly varied

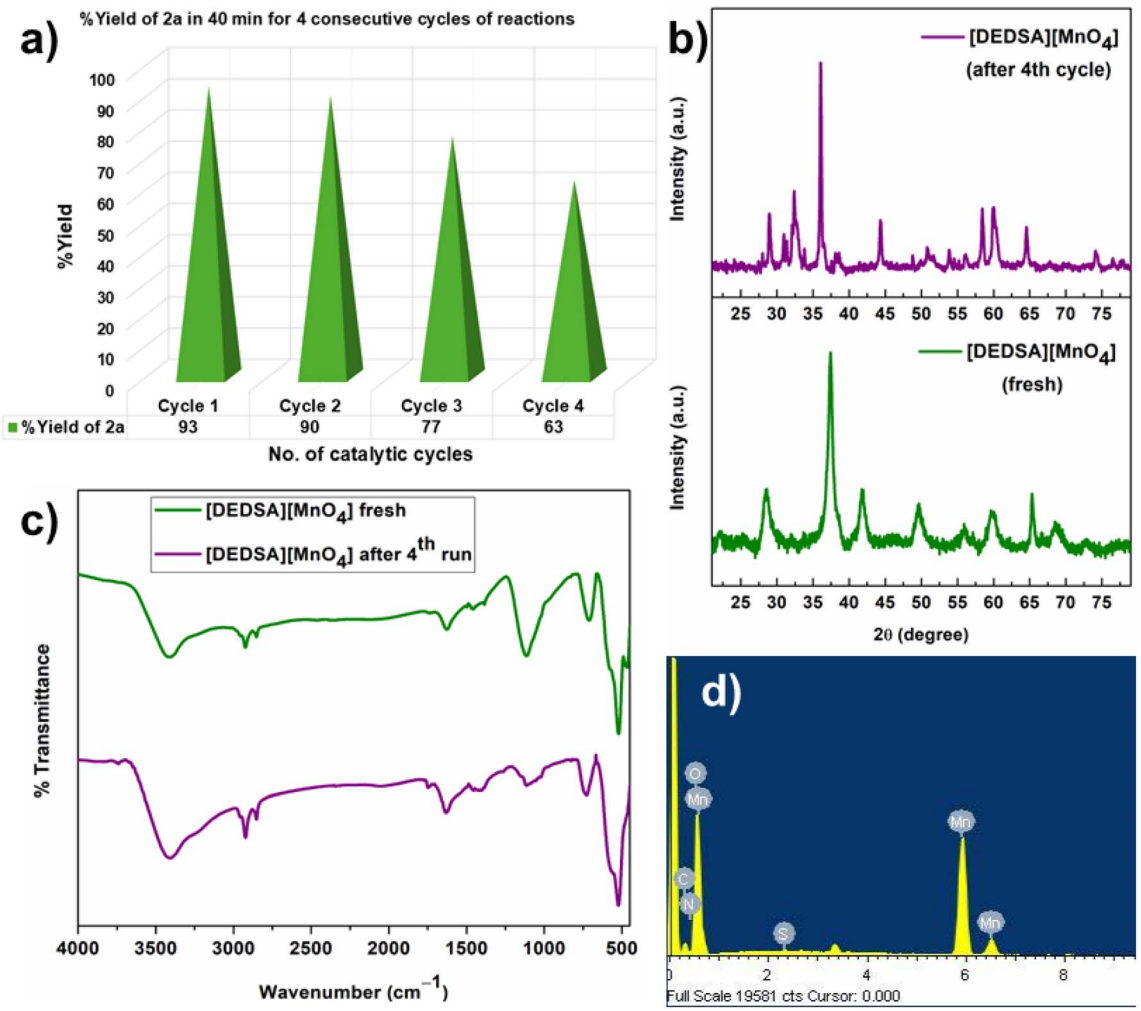

Fig. 8 (a) A bar diagram showing catalyst recyclability, (b) the PXRD spectrum of the reused catalyst, (c) the FT-IR spectrum of the reused catalyst, and (d) EDX analysis of the recovered catalyst.

intensities (Fig. 8c). EDX analysis depicted the presence of all the relevant elements in the recovered catalyst (Fig. 8d).

4. Conclusions

Two organic–inorganic hybrids of sulfonic-acid-functionalized ammonium- and piperazinium-based cations with permanganate anions were developed as sustainable oxidants by anion exchange reactions of $KMnO_4$ with the respective chloride-based ammonium salt precursors. The structural compositions and thermal stabilities of both hybrids were studied using FT-IR, SEM, EDX, UV-vis DRS, PXRD, and Raman techniques and TGA techniques, respectively. The oxidative power of these hybrids was examined through their use as an efficient oxidative catalyst for the selective oxidation of sulfides to sulfoxides in 10% aqueous sulfuric acid solution at 80 °C, where sulfuric acid acted as a co-catalyst. The [DEDSA][MnO_4] hybrid was also found to be recyclable for up to 4 cycles of sulfide oxidation reaction.

Data availability

The data that supports the findings of this study are available in the ESI† of this article.

Author contributions

Sangeeta Kalita: conceptualization, investigation, methodology, formal analysis, data curation, writing – original draft. Niharika Kashyap: investigation, visualization. Prapti Priyam Handique: investigation, validation. Debanga Bhusan Bora: visualization, validation. Ruli Borah: supervision, formal analysis, writing – review & editing.

Conflicts of interest

There are no conflicts to declare.

Acknowledgements

The authors appreciate the Sophisticated Analytical Instrumentation Centre (SAIC), Tezpur University for sample analysis. Special thanks to Dr Rajiv C. Dev Goswami, Guwahati Biotech Park, for GC-MS analysis.

References

1 G. Capozzi, S. Patai and Z. Rappoport, *The Syntheses of Sulphones, Sulphoxides and Cyclic Sulphides*, New York, 1994.
2 G. E. O'Mahony, A. Ford and A. R. Maguire, *J. Sulfur Chem.*, 2013, **34**, 301–334.
3 E. Wojaczynska and J. Wojaczynski, *Chem. Rev.*, 2010, **110**, 4303–4356.
4 R. Bentley, *Chem. Soc. Rev.*, 2005, **34**, 609–624.
5 I. Fernández and N. Khiar, *Chem. Rev.*, 2003, **103**, 3651–3706.
6 M. A. Fascione, S. J. Adshead and P. K. Mandal, *Chem.–Eur. J.*, 2012, **18**, 2987–2997.
7 M. C. Carreño, *Chem. Rev.*, 1995, **95**, 1717–1760.
8 C. Yang, Q. Jin and H. Zhang, *Green Chem.*, 2009, **11**, 1401–1405.
9 F. A. Cotton and R. Francis, *J. Am. Chem. Soc.*, 1960, **82**, 2986–2991.
10 D. A. Evans and G. C. Andrews, *Accounts Chem. Res.*, 1974, **7**, 147–155.
11 A. Regueiro-Ren, *Adv. Heterocycl. Chem.*, 2021, **134**, 1–30.
12 S. Q. Cai, K. F. Zhang and X. H. Cai, *Curr. Org. Chem.*, 2022, **26**, 91–121.
13 J. C. Xiang, Q. H. Gao and A. X. Wu, The Applications of DMSO, in *Solvents as Reagents in Organic Synthesis: Reactions and Applications*, Wiley-VCH Verlag GmbH & Co. KGaA publisher, ed. X.-F. Wu, 1st edn, 2018, pp. 315–353.
14 C. Kwak, J. J. Lee and J. S. Bae, *Appl. Catal., A*, 2000, **200**, 233–242.
15 R. Shafi and G. Hutchings, *Catal. Today*, 2000, **59**, 423–442.
16 X. Ma, K. Sakanishi and I. Mochida, *Ind. Eng. Chem. Res.*, 1994, **33**, 218–222.
17 D. Zhao, J. Wang and E. Zhou, *Green Chem.*, 2007, **9**, 1219–1222.
18 P. Kowalski, K. Mitka and K. Ossowska, *Tetrahedron*, 2005, **61**, 1933–1953.
19 V. G. Shukla, P. D. Salgaonkar and K. G. Akamanchi, *J. Org. Chem.*, 2003, **68**, 5422–5425.
20 P. J. Kropp, G. W. Breton and J. D. Fields, *J. Am. Chem. Soc.*, 2000, **122**, 4280–4285.
21 N. Iranpoor, H. Firouzabadi and A. R. Pourali, *Synlett*, 2004, **2004**, 0347–0349.
22 N. M. Andrijashina, N. Alexandr, A. N. Lobov, A. V. Antipin and R. L. Safiullin, *Synlett*, 2023, **34**, 1247–1252.
23 S. Wang, L. Tang, B. Cai, Z. Yin, Y. Li, L. Xiong, X. Kang, J. Xuan, Y. Pei and M. Zhu, *J. Am. Chem. Soc.*, 2022, **144**, 3787–3792.
24 M. Forchetta, F. Sabuzi, L. Stella, V. Conte and P. Galloni, *J. Org. Chem.*, 2022, **87**, 14016–14025.
25 F. Armandsefat, S. Hamzehzadeh and N. Azizi, *Sci. Rep.*, 2024, **14**, 12614.
26 F. Armandsefat, S. Hamzehzadeh, N. Azizi and B. S. Chalaki, *Curr. Opin. Green Sustainable Chem.*, 2024, **8**, 100414.
27 P. Kowalski, K. Mitka and K. Ossowska, *Tetrahedron*, 2005, **61**, 1933–1953.
28 B. Zhang, M. D. Zhou and M. Cokoja, *RSC Adv.*, 2012, **2**, 8416–8420.
29 D. Zhao, Y. Wang and E. Duan, *Fuel Process. Technol.*, 2010, **91**, 1803–1806.
30 X. B. Liu, Q. Rong and J. Tan, *Front. Chem.*, 2022, **9**, 798603.
31 M. Zhang, W. Zhu and S. Xun, *J. Chem. Eng.*, 2013, **220**, 328–336.
32 W. Zhu, H. Li and X. Jiang, *Energy Fuels*, 2007, **21**, 2514–2516.
33 R. Fareghi-Alamdari, N. Zekri and A. Moghadam, *Catal. Commun.*, 2017, **98**, 71–75.
34 C. J. Carrasco, F. Montilla and E. Álvarez, *Dalton Trans.*, 2014, **43**, 13711–13730.
35 P. Zhao, M. Zhang and Y. Wu, *Ind. Eng. Chem. Res.*, 2012, **51**, 6641–6647.

36 K. P. Bryliakov and E. P. Talsi, *Curr. Org. Chem.*, 2012, **16**, 1215–1242.
37 N. J. Leonard and C. R. Johnson, *J. Org. Chem.*, 1962, **27**, 282–284.
38 M. K. Panda, M. M. Shaikh and P. Ghosh, *Dalton Trans.*, 2010, **39**, 2428–2440.
39 H. Gan, C. Qin and L. Zhao, *Cryst. Growth Des.*, 2012, **21**, 1028–1034.
40 S. Dash, S. Patel and B. K. Mishra, *Tetrahedron*, 2009, **65**, 707–739.
41 F. G. Bordwell and G. D. Cooper, *J. Am. Chem. Soc.*, 1952, **74**, 1058–1060.
42 K. K. Banerji, *Tetrahedron*, 1988, **44**, 2969–2975.
43 D. G. Lee and T. Chen, *J. Org. Chem.*, 1991, **56**, 5346–5348.
44 A. Shaabani, F. Tavasoli-Rad and D. G. Lee, *Synth. Commun.*, 2005, **35**, 571–580.
45 A. Jayaraman and A. L. East, *J. Org. Chem.*, 2012, **77**, 351–356.
46 A. Hajipour, S. Mallakpour and H. Adibi, *Sulfur Lett.*, 2002, **25**, 155–160.
47 A. Shaabani, P. Mirzaei and D. G. Lee, *Catal. Lett.*, 2004, **97**, 119–123.
48 A. Shaabani, A. Rahmati and M. Sharifi, *Chem. Mon.*, 2007, **138**, 649–651.
49 A. Shaabani, A. Bazgir and D. G. Lee, *Synth. Commun.*, 2004, **34**, 3595–3607.
50 A. Acharjee, M. A. Ali and B. Saha, *J. Solution Chem.*, 2018, **47**, 1449–1478.
51 H. J. Schmidt and H. J. Schäfer, *Angew. Chem., Int. Ed. Engl.*, 1979, **18**, 787.
52 D. Scholz, *Chem. Mon.*, 1981, **112**, 241–243.
53 L. A. Paquette, *Encyclopaedia of Reagents for Organic Synthesis*, Chichester, 2nd edn, 2009.
54 H. Karaman, *PhD Thesis*, University of Regina, 1982.
55 M. M. Lakouraj, M. Tajbakhsh and H. Tashakkorian, *Phosphorus Sulfur Silicon Relat. Elem.*, 2007, **182**, 485–490.
56 P. Sarma, A. K. Dutta and R. Borah, *Catal. Surv. Asia*, 2017, **21**, 70–93.
57 S. Das, N. Kashyap and S. Kalita, *Adv. Phys. Org. Chem.*, 2020, **54**, 1–98.
58 R. Giernoth, *Angew. Chem., Int. Ed.*, 2010, **49**, 2834–2839.
59 S. K. Singh and A. W. Savoy, *J. Mol. Liq.*, 2020, **297**, 112038.
60 N. Kashyap, S. Das and R. Borah, *Polyhedron*, 2021, **196**, 114993.
61 S. Kalita, N. Kashyap and D. B. Bora, *ChemistrySelect*, 2023, **8**, 202204533.
62 A. K. Dutta, P. Gogoi and R. Borah, *Appl. Organomet. Chem.*, 2018, **32**, 3900.
63 T. G. Koodehi, F. Shirini and O. Goli-Jolodar, *J. Iran. Chem. Soc.*, 2017, **14**, 443–456.
64 R. K. Khanna and D. D. Stranz, *Spectrochim. Acta, Part A*, 1980, **36**, 387–388.
65 P. J. Hendra, *Spectrochim. Acta, Part A*, 1968, **24**, 125–129.
66 A. Viste and H. B. Gray, *Inorg. Chem.*, 1964, **3**, 1113–1123.
67 I. Tanabe, Y. Kurawaki and Y. Morisawa, *Phys. Chem. Chem. Phys.*, 2016, **18**, 22526–22530.
68 C. Engert and W. Kiefer, *J. Raman Spectrosc.*, 1991, **22**, 715–719.
69 M. Thommes, K. Kaneko, A. V. Neimark, J. P. Olivier, F. Rodriguez-Reinoso, J. Rouquerol and K. S. Sing, *Pure Appl. Chem.*, 2015, **87**, 1051–1069.
70 Y. L. Hu, D. Fang and R. Xing, *RSC Adv.*, 2014, **4**, 51140–51145.
71 A. R. Hajipour, L. Khazdooz and A. E. Ruoho, *Phosphorus Sulfur Silicon Relat. Elem.*, 2009, **184**, 705–711.
72 S. Hussain, D. Talukdar, S. K. Bharadwaj and M. K. Chaudhuri, *Tetrahedron Lett.*, 2012, **53**, 6512–6515.
73 X. D. Li, R. Ma and L. N. He, *Chin. Chem. Lett.*, 2015, **26**, 539–542.
74 P. Veerakumar, Z. Z. Lu, M. Velayudham, K. L. Lu and S. Rajagopal, *J. Mol. Catal. A: Chem.*, 2010, **332**, 128–137.